JOURNAL OF PROPULSION AND POWER
Vol. 24, No. 6, November–December 2008

Laser-Assisted Combustion of Solid Propellant at Low Pressures

Akira Kakami* and Ryoma Hiyamizu†
Kyushu Institute of Technology, Kitakyushu 804-8550, Japan
Kiyotaka Shuzenji‡
Fukuoka Industrial Technology Center, Kitakyushu 807-0831, Japan
and
Takeshi Tachibana§
Kyushu Institute of Technology, Kitakyushu 804-8550, Japan

DOI: 10.2514/1.36458

This paper describes experimental work on laser-assisted combustion and its use to control solid propellants. Burning rates of hydroxyl-terminated polybutadiene and ammonium perchlorate composite solid propellants were measured at pressures up to 90 kPa under laser irradiation, and propellant-preheat temperature distribution was measured by thermography. Combustion control, including ignition and interruption by laser irradiation, was feasible with custom-made (fuel-rich) non-self-combustible solid propellants with a burning rate coincident with Vieille's law and a pressure exponent of approximately 0.5. Consequently, this combustion-control concept seems to be applicable to a microsatellite thruster. The heat balance on the burning surface evaluated at a laser power density of 1.4 $W \cdot mm^{-2}$ at 50 kPa produced the following results: chemical reaction was endothermic at a heat flux of -0.7 $W \cdot mm^{-2}$, heat was supplied to the solid phase of the propellant at a heat flux of 3.7 $W \cdot mm^{-2}$, and heat-feedback rate to the burning surface was 3.0 $W \cdot mm^{-2}$, which suggests that approximately 70% of the energy transferred to the burning surface was provided by combustion itself, and the laser supplied supplementary heat flux to compensate for the heat insufficiency to sustain combustion.

Nomenclature

a_L, b_L	=	coefficients defined in Eq. (1)
C	=	specific heat, $J/kg \cdot K$
I_f	=	radiant heat-feedback rate from the flame to the burning surface, $W \cdot mm^{-2}$
I_L	=	laser power density on the burning surface of the solid propellant, $W \cdot mm^{-2}$
n	=	pressure exponent
P	=	pressure, Pa
Q	=	heat of the reaction, kJ/kg
r	=	burning rate, m/s
$r\rho_p Q_s$	=	heat intensity of the reaction on the burning surface, $W \cdot mm^{-2}$
T	=	temperature, K
t	=	time
x	=	moving coordinate for which the origin is fixed at the burning surface, m
Λ_g	=	conductive heat-feedback rate from the gas phase to the burning surface, $W \cdot mm^{-2}$
$\Lambda_g + I_f$	=	heat-feedback rate from the flame to the burning surface, $W \cdot mm^{-2}$
Λ_p	=	heat flux supplied from the burning surface to the solid phase of the solid propellant, $W \cdot mm^{-2}$
λ	=	thermal conductivity, $W \cdot m^{-1} \cdot K^{-1}$
ρ_p	=	mass density of the solid propellant, $kg \cdot m^{-3}$

Subscripts

g	=	gas phase
p	=	solid-phase propellant
s	=	burning surface
0	=	initial condition

Presented as Paper 5783 at the 43rd AIAA/ASME/SAE/ASEE Joint Propulsion Conference and Exhibit, Cincinnati, OH, 8–11 July 2007; received 4 January 2008; revision received 23 July 2008; accepted for publication 29 July 2008. Copyright © 2008 by the American Institute of Aeronautics and Astronautics, Inc. All rights reserved. Copies of this paper may be made for personal or internal use, on condition that the copier pay the $10.00 per-copy fee to the Copyright Clearance Center, Inc., 222 Rosewood Drive, Danvers, MA 01923; include the code 0748-4658/08 $10.00 in correspondence with the CCC.

*Assistant Professor, Department of Mechanical Engineering. Member AIAA.
†Former graduate student, Department of Mechanical Engineering.
‡Senior Engineer, Mechanics and Electronics Research Institute. Member AIAA.
§Professor, Department of Mechanical Engineering. Senior Member AIAA.

I. Introduction

A SOLID-PROPELLANT thruster is one of the potential options for a small space-propulsion device such as a microthruster for a microsatellite, because its relatively simple structure makes it possible to downsize a satellite. A microsatellite is compact and lightweight compared with conventional satellites. A microsatellite has been developed and flown successfully in low Earth orbit; however, it had no thruster and was restricted to a ballistic flight, partially due to the size of the conventional thruster. A microthruster requires a suitable thruster for microsatellite missions.

A solid-propellant thruster, however, presents difficulties related to starting, firing interruption, and thrust variations. Once the solid propellant is ignited, combustion is sustained autonomously until all of the propellant is consumed [1].

In this study, using our original non-self-combustible solid propellant, laser-assisted combustion was tested for combustion control. Figure 1 is a conceptual diagram showing how combustion is started by directing a laser beam onto the solid-propellant surface and how combustion is interrupted by cutting off the laser.

With a conventional solid propellant, combustion is generally sustained autonomously and is uncontrollable; however, combustion can be controlled with the non-self-combustible solid propellant by adding heat flux. We previously showed that solid-propellant combustion was sustained during an arc discharge and was extinguished by turning off the discharge current [2]. A 1 kW arc

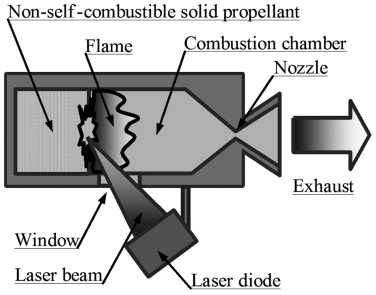

Fig. 1 Conceptual diagram of the proposed thruster.

discharge successfully controlled a 1-N-class thrust, although less power would be necessary for small thrusters.

A laser diode is one of the preferred heat sources for combustion control in a lower-power-level thruster. A laser diode is compact and lightweight, and the operating voltage is as low as 5 V. The laser has an energy-conversion efficiency of more than 50% for a beam power of 1 mW to 1000 W, which is compatible with the thruster power level and is easily available. Laser power can be varied easily by adjusting the driving current.

There are various studies on the application of lasers to the solid propellants. The following studies explore thruster development and propellant combustion/decomposition modeling. Koizumi et. al. [3] implemented laser diodes for K/BNO_3 [3] propellant ignition and evaluated the thruster performance. Esker and Brewster [4] conducted studies using laser pyrolysis with hydroxyl-terminated polybutadiene (HTPB) for hybrid propulsion systems. Li and Litzinger [5] investigated butanetriol trinitrate and glycidyl azide polymer combustion under laser radiation to obtain a quantitative species profile through the use of a triple-quadrupole mass spectrometer.

This paper will focus on laser-assisted combustion of a solid propellant. We developed a test to evaluate the feasibility of our original thruster concept and to document the fundamental characteristics. Burning rates were measured with laser power densities ranging from 0.5 to 1.4 $W \cdot mm^{-2}$. Temperature distribution on the solid-propellant surface was measured two-dimensionally using high-resolution thermography. Heat balance on the burning surface was evaluated using the data obtained from the burning rates and the solid-propellant temperature distribution.

II. Experimental Apparatus

A. Vacuum Chamber

A diagram of the apparatus is given in Fig. 2. All of the test propellants were tested in a $350 \times 350 \times 350$ mm vacuum chamber with a 300-mm-diam window for monitoring propellant combustion with a digital charge-coupled device (CCD) camera and a 100-mm-diam window for introducing the laser beam.

The vacuum chamber was connected to two valves: an exhaust valve connected to a rotary pump of 240 liter/ min in evacuation velocity and a nitrogen valve connected to a nitrogen tank through a pressure regulator. The chamber pressure was kept at the target value by adjusting the valves. Chamber pressure was variable from 3 to 90 kPa.

Before laser irradiation, using a rotary pump, the vacuum chamber was evacuated down to 1 kPa, and then nitrogen was supplied to eliminate the influence of oxygen in the air. During laser irradiation, the chamber pressure was monitored with a pressure transducer and was kept at the target value by adjusting the valves.

B. Laser

A 50-W-class continuous-wave Nd:YAG laser (Lee Laser, Inc., 7150M-200) was used as a tentative alternative to a laser diode. The experimental results using the YAG laser are the same as those obtained with a laser diode. A YAG laser is comparable with a watt-class laser diode in beam wavelength, power density, and power level. Both lasers are identical in terms of laser power adsorbed by propellant and absorption depth.

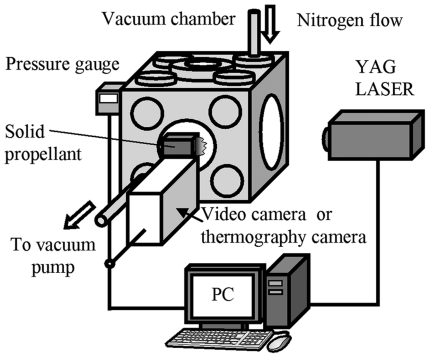

Fig. 2 Experimental setup.

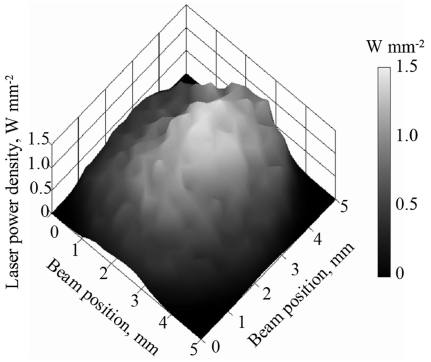

Fig. 3 Laser-power-density distribution.

The laser used in the tests was a flash-lamp-pumped YAG laser emitting a multi-transverse-mode beam of 1064 nm in wavelength. Figure 3 shows the laser-power-density distribution of the YAG laser measured using a photo diode.

Laser power density was adjusted with $30 \times 10 \times 1$ mm rectangular glass slides. The glass slides, which transmitted approximately 70% of the laser beam per single slide, were located between the YAG laser and the laser-introducing window of the vacuum chamber. The slides were ordinary silica glass without special doping or antireflection coating and attenuated the laser beam by reflection. By adjusting the number of glass slides, the laser power density provided to the solid-propellant surface was varied from 0.75 to 1.4 $W \cdot mm^{-2}$.

C. Solid Propellant

Table 1 lists the solid propellants used in the experiment. The test propellants were all fuel-rich composite solid propellants made of HTBP and ammonia perchlorate (AP). The average diameter of an

Table 1 Ingredients and weight mixture ratio of test solid propellants

Test propellant	HTPB	AP	Carbon black	Aluminum
1	30	70	0.5	——
2	40	60	0.5	——
3	50	50	0.5	——
4	30	70	5	——
5	40	60	5	——
6	50	50	5	——
7	30	70	——	0.5
8	40	60	——	0.5
9	50	50	——	0.5
10	30	70	——	5
11	40	60	——	5
12	40	60	0.1	0.5
13	40	60	0.1	5

AP particle was approximately 5 μm. Additives such as carbon black and aluminum were supplemented to augment laser beam absorption. In our previous study, HTPB/AP propellants with no additives did not ignite even after 60-s laser irradiation [6]. In contrast, solid propellants with additives such as titanium, aluminum, or carbon black were ignited by laser irradiation. This could be due to the difference in the near-infrared absorptivity or the absorption depth of the additives. Hence, a solid propellant with carbon black and aluminum additives was used throughout the experiments. The particle sizes of the aluminum and carbon black were 20 and 3 μm, respectively, and their respective volumetric concentrations were 0.35 and 0.5% in the typical case of 0.5 wt % additives. The propellants used in this study were all made by Asahi Kasei Chemicals Corporation, one of the three major propellant manufacturers in Japan. It has been reported by the company that particles were added using their routine mixing method and that their distribution uniformity was assured and even better than ordinary propellants because these non-self-combustible propellants include more binder and therefore mix better.

The test propellants were typically $2 \times 2 \times 20$ mm rectangular bars. The size of the cross section was determined from the laser-power-density distribution. As shown in Fig. 3, the laser power density was found to be sufficiently uniform in the vicinity of the laser beam center. In all tests, the end of the test propellant was aligned so that the 2×2 mm solid bar surface was irradiated with a uniform laser power density. The standard deviation of the laser power density on the laser-irradiated surface of the solid-propellant bar was 0.1 $\mathrm{W \cdot mm^{-2}}$ at a laser power density of 1.4 $\mathrm{W \cdot mm^{-2}}$.

D. Burning-Rate Measurement

The flame and solid-propellant regression behaviors were recorded at a frame rate of 30 Hz with a digital CCD video camera from a lateral view, as shown in Fig. 2. Burning rates were evaluated from the images. A personal computer captured motion pictures from the digital CCD video camera and calculated the burning-surface position on each frame by comparing the brightness along the longitudinal axis of the solid-propellant bar. The burning-surface position was expressed as a function of time, and the burning rates were determined using the least-squares method.

E. Infrared Thermograph Measurement of the Solid-Propellant Surface

Temperature distribution on the solid-propellant surface along the longitudinal axis was measured with a thermography camera (Chino Corporation, CAP-8200) from a lateral view, as shown in Fig. 2. Using a macrolens, the thermograph camera measures surface temperature distribution in the range from 273 to 773 K, with a temperature resolution of 0.08 K for an area of 5.7×4.3 mm and at a spatial resolution of 18 μm. Because the thermography camera detected far-infrared emissions of 7.5 to 13 mm in wavelength, a germanium glass with a transmission ratio of approximately 50%, which was almost uniform at wavelengths ranging from 2 to 14 μm, was used for the observation window to measure temperature distribution. To compensate for attenuation caused by the germanium window of the test chamber, in situ calibration for the temperature measurement was conducted with a K-type thermocouple approximately 0.8 mm in diameter, coated with a carbon-black-based spray set at the position of the solid propellant and heated with a glow plug set a few millimeters beneath. The temperatures were compared with those obtained by the thermography camera at 10 elevated temperatures. The calibration curve obtained with this method showed that they were proportional to each other, with a standard-deviation-based error of 5.8 K in the temperature measurement.

III. Results and Discussion

A. Observation of the Solid-Propellant Combustion

Figures 4 and 5 show images of combustion using test propellant 1 and a time history of the burning-surface position, respectively. Time

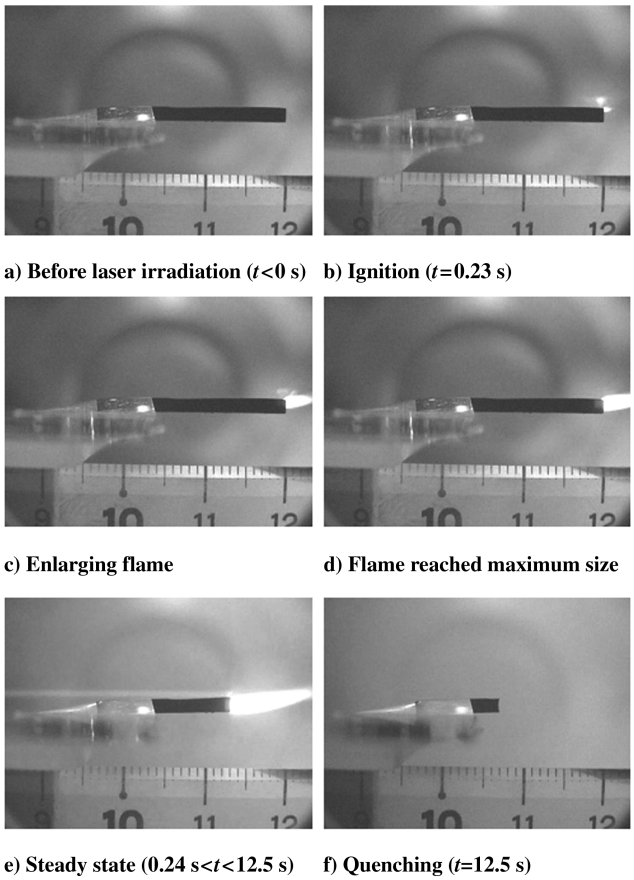

a) Before laser irradiation ($t<0$ s) **b) Ignition ($t=0.23$ s)**

c) Enlarging flame **d) Flame reached maximum size**

e) Steady state (0.24 s$<t<$12.5 s) **f) Quenching ($t=12.5$ s)**

Fig. 4 Images of propellant combustion using test propellant 1.

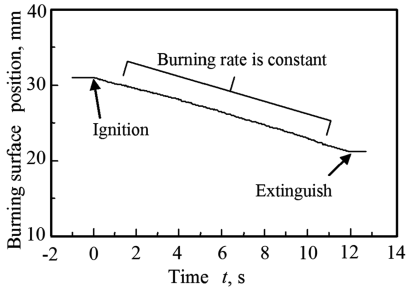

Fig. 5 Time history of the burning-surface position.

origin $t = 0$ is defined as the instant when the laser radiation was started. The test propellant was irradiated with a laser of 1.4 $\mathrm{W \cdot mm^{-2}}$ power density at a chamber pressure of 50 kPa. In Fig. 4, irradiation of the solid propellant started at $t = 0$. The red line above the solid propellant is a milliwatt-class He-Ne laser used for aligning the YAG laser and had an insignificant influence on combustion. At $t = 0.23$ s, a small initial flame is found in the image, which grew rapidly and finally reached its maximum size within 0.1 s. Combustion was sustained stably, with the flame neither flickering nor being extinguished during laser irradiation. The solid propellant regressed in parallel with the initial solid-propellant surface along the longitudinal axis. At the instant that laser irradiation was interrupted, the flame began to shrink rapidly and the solid propellant was extinguished. After interrupting laser irradiation, the flame remained extinguished until laser irradiation was restarted. This result verifies that combustion of the solid propellant was good, with laser irradiation controlling starting and interruption with an ignition delay of 0.23 s. As shown in Fig. 5, the burning surface regressed at a constant rate, and combustion could be successfully controlled at pressures ranging from 3 to 90 kPa, with a laser power density of 0.7 to 1.4 $\mathrm{W \cdot mm^{-2}}$ using all of the test propellants tested.

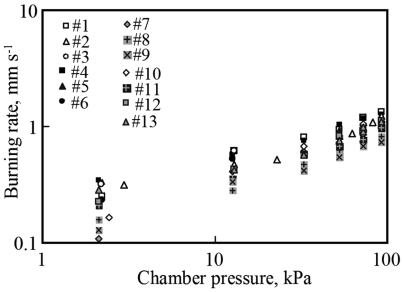

Fig. 6 Dependence of the burning rate on chamber pressure with a laser power density of 1.4 W · mm^{-2}.

B. Burning Rate

The burning rate was measured at chamber pressures ranging from 3 to 90 kPa, with a laser power density of 1.4 W · mm^{-2}. Because observations using the CCD camera showed that the burning surface regressed at nearly a constant rate in all of the tests, as shown in Fig. 5, the burning rate was determined from the burning surface. Figure 6 shows the relation between chamber pressure and burning rate. Pressure exponents and temperature coefficient were evaluated by fitting the data using Vieille's law $r = aP^n$, where r is the burning rate (mm/s) and P is pressure (kPa). As shown in Table 2, the pressure exponent ranged from 0.28 to 0.53 for all test propellants, which indicates that our proposed method is applicable for controlling solid-propellant combustion.

C. Laser Power Density

Figure 7 shows the dependence of the burning rate on applied laser power density in the case of test propellant 1. At any chamber pressure, the burning rate is proportional to laser power density. Using the least-squares method, the data were fitted with the linear equation

$$r = a_L I_L + b_L \tag{1}$$

Table 3 shows the coefficients a_L and b_L evaluated at each chamber pressure, for which $r = a_L I_L + b_L$. r is the burning rate and I_L is the laser power density.

The heat-feedback rate to the burning surface $(I_f + \Lambda_g)$ is evaluated from the relation between laser power density and burning rate. A heat-balance equation for the burning surface has been proposed and used to analyze the combustion of the solid propellant [7]. For combustion under laser irradiation, the heat input term of the laser, I_L, is added to the heat-balance equation. Figure 8 is a schematic of the heat-balance model under laser irradiation. The heat balance on the burning surface under laser irradiation is expressed as

$$\Lambda_p = \rho_p r Q_s + \Lambda_g + I_f + I_L \tag{2}$$

In the solid-phase area of the solid propellant, the heat transfer equation using a moving coordinate x, for which the origin is taken at the burning surface, is expressed by the equation

$$\lambda_p \frac{d^2T}{dx^2} - \rho_p C_p r \frac{dT}{dx} = 0 \tag{3}$$

with the boundary conditions

$$T = T_0 \quad \text{at } x = -\infty \qquad T = T_s \quad \text{at } x = 0$$

Integrating Eq. (3) with x, the heat flux from the burning surface to the solid phase Λ_p is expressed by

$$\Lambda_p = \lambda_p \left(\frac{dT}{dx}\right)_{s-} = C_p \rho_p r (T_s - T_0) \tag{4}$$

Substituting Eq. (4) into Eq. (2), the burning rate r is expressed by

$$r = \frac{1}{C_p \rho_p (T_s - T_0) - \rho_p Q_s} I_L + \frac{\Lambda_g + I_f}{C_p \rho_p (T_s - T_0) - \rho_p Q_s} \tag{5}$$

The experimental results show that the burning rate is linear with laser power density at a constant chamber pressure, as shown in Fig. 7. Comparing Eq. (1) with Eq. (5), the values a_L and b_L are expressed by

$$a_L = \frac{1}{C_p \rho_p (T_s - T_0) - \rho_p Q_s} \tag{6}$$

$$b_L = \frac{\Lambda_g + I_f}{C_p \rho_p (T_s - T_0) - \rho_p Q_s} \tag{7}$$

and the values a_L and b_L are constant in the case with a fixed chamber pressure. From Eqs. (6) and (7), the heat-feedback rate to the burning surface $(\Lambda_g + I_f)$ is obtained with the equation

Table 2 Burning rate for each test propellant with a laser power density of 1.4 W · mm^{-2}

Test propellant	Temperature coefficient a	Pressure exponent n	Relation coefficient R^2
1	0.185	0.43	0.99
2	0.186	0.39	0.95
3	0.262	0.28	0.95
4	0.251	0.35	0.98
5	0.255	0.31	0.99
6	0.189	0.34	0.96
8	0.105	0.44	0.98
9	0.095	0.45	0.99
10	0.105	0.53	1.00
11	0.146	0.40	0.98
12	0.160	0.41	0.99
13	0.194	0.35	0.94

Table 3 Evaluated coefficients for laser power density with test propellant 1

Chamber pressure, kPa	Coefficient a_L	Coefficient b_L	Correlation coefficient R^2
30	0.23	0.41	0.91
50	0.20	0.61	1.0
90	0.14	1.01	0.91

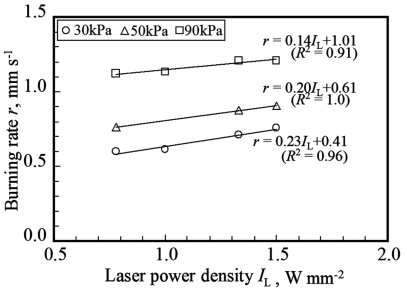

Fig. 7 Dependence of the burning rate on laser power density using test propellant 1.

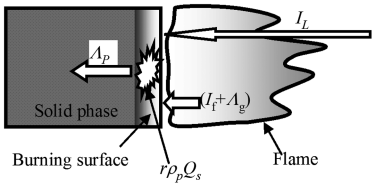

Fig. 8 Heat-balance model on the burning surface.

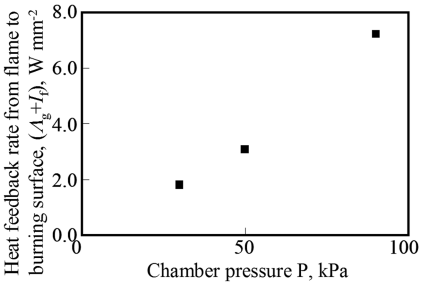

Fig. 9 Relationship between chamber pressure and heat-feedback rate to the burning surface ($\Lambda_g + I_f$).

$$\Lambda_g + I_f = \frac{b_L}{a_L} \tag{8}$$

Using the experimental results shown in Table 3, the value of $\Lambda_g + I_f$ is calculated with Eq. (8). Figure 9 shows the relation between chamber pressure and heat-feedback rate to the burning surface ($\Lambda_g + I_f$). The value of $\Lambda_g + I_f$ is larger by factors of 1.3, 2.0, and 5.2 than laser power density I_L of 1.4 W · mm^{-2} at chamber pressures of 30, 50, and 90 kPa, respectively. These results mean that during laser-assisted combustion of the solid propellant, the heat feedback provided much, but not all, of the energy required to sustain combustion. The laser supplied some supplementary heat to the burning surface and compensated for the lack of heat flux to sustain combustion.

D. Solid-Propellant-Surface Temperature Distribution and Heat Balance on the Burning Surface

The temperature of the solid-propellant side surface was measured by high-resolution thermography. Figure 10 shows a typical two-dimensional temperature distribution measured under the condition of laser power density of 1.4 W · mm^{-2} and chamber pressure of 50 kPa. Because the distribution in Fig. 10 was obtained after the burning rate became constant, the figure shows the temperature distribution in a steady state. The gas-phase temperature ($x > 0$) does not display true values because the emissivity of the exhaust is unknown, due to the complexity of the mixture of exhaust gas. In the solid-phase region ($x < 0$), the temperature distribution is quasi-one-dimensional. Figure 11 shows the temperature distribution along the x axis shown in Fig. 10. The temperature rises steadily as x increases in the solid phase, and the highest temperature is burning-surface

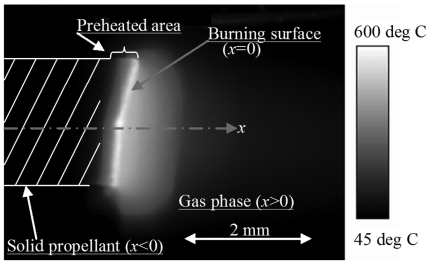

Fig. 10 Temperature distribution of the solid-propellant test propellant 1 at 50 kPa with a laser power density of 1.4 W · mm^{-2}.

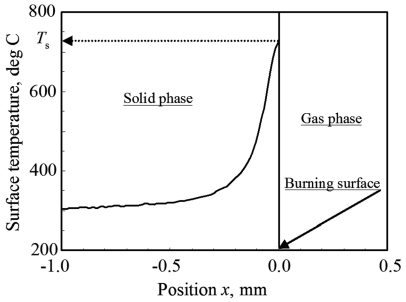

Fig. 11 Temperature distribution along the x axis with test propellant 1 at 50 kPa with a laser power density of 1.4 W · mm^{-2}.

temperature T_s. During laser irradiation, burning-surface temperature T_s was kept at approximately 730 K, which is approximately equal to the melting point of ammonium perchlorate.

Regarding the transient state after starting laser irradiation, burning-surface temperature T_s increased with time and finally reached a constant value of 730 K. The solid propellant (with an initial temperature of $T_s = 295$ K) irradiation started at $t = 0$, and surface temperature increased steadily. At $t = 0.23$ s, the solid propellant was ignited at $T_s = 536$ K, and after ignition, the temperature continued to increase to a final stable value of 730 K.

Figure 12 shows the relationship between burning-surface temperature in steady state T_s and laser power density I_L at a chamber pressure of 50 kPa using test propellant 1. The surface temperature T_s appears to be almost independent of laser power density.

Using the values determined for T_s and $\Lambda_g + I_f$, the heat balance on the burning surface was evaluated for the case with test propellant 1 at 50 kPa at $I_L = 1.4$ W · mm^{-2}. At burning-surface temperature $T_s = 730$ K, the heat supplied to the solid phase Λ_p was determined to be 3.7 W · mm^{-2} by Eq. (4).

Substituting the evaluated values of Λ_P and $(\Lambda_g + I_f)$ and laser power density $I_L = 1.4$ W · mm^{-2} into Eq. (2), the heat intensity of the reaction on the burning surface $r\rho_p Q_s$ is found to be -0.7 W · mm^{-2}. As shown in Fig. 6, the burning rate r of the test propellant 1 was 1.0 mm/s. The reaction heat on the burning surface Q_s is found to be -43 kJ/kg. This result shows that the chemical reaction on the solid-propellant surface was endothermic. The energy balance on the burning surface is summarized from those

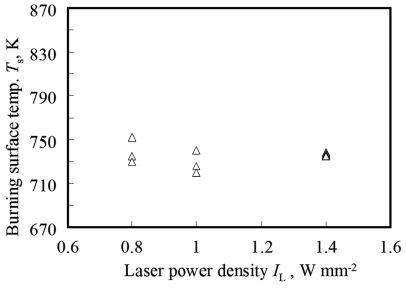

Fig. 12 Relationship between laser power density and burning-surface temperature.

results as follows, with a chamber pressure of 50 kPa, test propellant 1, and evaluated values at $W \cdot mm^{-2}$: laser power density was $I_L = 1.4$, the heat-feedback rate to the burning surface was $\Lambda_g + I_f = 3.0$, the heat intensity of the reaction on the burning surface was $r\rho_p Q_s = -0.7$, and the heat supply to the solid phase of propellant was $\Lambda_p = 3.7$ (the positive value shows that the heat is provided to the solid-propellant surface).

An estimation based on a forced-convection heat transfer model showed that the heat-loss rate through the sides of the sample had a negligible influence on the heat-balance calculation. In this model, the burning propellant had two separate zones: a thin zone heated by the neighboring burning surface (preheated zone) and a cold zone kept at the initial temperature. The calculation yielded a heat-loss rate of 0.013 W, assuming that the preheated zone with a thickness of 0.15 mm had a uniform temperature of 730 K (which was obtained by thermography) and that the propellant temperature in the cold zone T_0 was the same as that of the nitrogen flow. This heat-loss rate is still overestimated because the real temperature exponentially decreased in the preheated zone, as shown in Fig. 11. This heat-loss rate is negligibly small, even when compared with the heat-production rate of the reaction (−2.8 W) obtained as the product of the burning area and $r\rho_p Q_s$.

IV. Conclusions

With some HTPB/AP-based composite solid propellants, which were specially made to be non-self-combustible, combustion control was successful with laser irradiation at pressures ranging from 3 to 90 kPa. Adding carbon-black powder to the solid propellant led to a reduced ignition delay of 0.23 s. Measurement with a digital CCD camera revealed that the burning-rate pressure exponent n stayed in the range from 0.4 to 0.6, which verifies that the laser-assisted combustion method for a solid propellant is applicable to a small thruster with full combustion control.

The heat balance on the burning surface was evaluated from the burning rates and burning-surface temperature. From the theoretical heat balance on the burning surface, the heat-feedback rate to the burning surface ($\Lambda_g + I_f$), the heat flux to the solid phase Λ_p, and the heat intensity of the reaction on the burning surface $r\rho_p Q_s$ were determined from the relationship between burning rate and laser power density in the case that T_s was determined from measurements. Thermography showed that the burning-surface temperature T_s in a steady state was 730 K and was independent of laser power density at 50 kPa in the case with test propellant 1. With a laser power density of 1.4 $W \cdot mm^{-2}$, the values of ($\Lambda_g + I_f$), $r\rho_p Q_s$, and Λ_p were 3.0, −0.7, and 3.7 $W \cdot mm^{-2}$, respectively. Using a burning rate of 1.0 mm/s and the mass density of the propellant, the reaction heat on the burning surface Q_s was −43 kJ/kg, which showed that the chemical reaction on the burning surface was endothermic.

At 90 kPa, burning-rate measurements with the laser power densities ranging from 0.7 to 1.4 $W \cdot mm^{-2}$ yielded the heat-feedback rate to the burning surface ($\Lambda_g + I_f$) of 7.8 $W \cdot mm^{-2}$. Overall, under laser-assisted combustion, the energy-sustaining combustion of the solid propellant was mostly supplied by combustion heat; the laser supplied supplementary heat to the burning surface and compensated for the insufficiency of the heat flux for sustaining combustion. Hence, a solid-propellant thruster using laser-sustained combustion can be categorized as chemical propulsion.

Acknowledgments

This work was partially supported by Grant-in-Aid for Scientific Research (B) no. 17360411 by the Japan Society for the Promotion of Science (JSPS). The authors also acknowledge Asahi Kasei Chemicals Corporation for supplying the propellant.

References

[1] Sutton, G. P., and Biblarz, O., *Rocket Propulsion Elements*, 7th ed., Willey-Interscience, New York, 2000, Chaps. 11, 14.

[2] Tachibana, T., and Ohisa, H., "Electrical Combustion Control of AP- and AN-Based Propellants for Upper Stage Applications," *Journal of Propulsion and Power*, Vol. 15, No. 6, 1999, pp. 874–879. doi:10.2514/2.5510

[3] Koizumi, H., Inoue T., Arakawa, Y., and Nakano, M., "Dual Propulsive Mode Microthruster Using a Diode Laser," *Journal of Propulsion and Power*, Vol. 21, No. 6, 2005, pp. 1133–1136. doi:10.2514/1.13221

[4] Esker, D. R., and Brewster, M. Q., "Laser Pyrolysis of Hydroxyl-Terminated Polybutadiene," *Journal of Propulsion and Power*, Vol. 12, No. 2, 1996, pp. 296–301. doi:10.2514/3.24027

[5] Li, J., and Litzinger T. A., "Laser-Driven Decomposition and Combustion of BTTN/GAP," *Journal of Propulsion and Power*, Vol. 23, No. 1, 2007, pp. 166–174. doi:10.2514/1.20293

[6] Kakami, A., Masaki S., .Horisawa H., and Tachibana T., "Solid Propellant Microthruster Using Laser-Assisted Combustion," 40th AIAA/ASME/SAE/ASEE, Joint Propulsion Conference and Exhibit, AIAA Paper 2004-3797, 2004.

[7] De Luca, L., Price, W. E., and Summerfield, M. (ed.), *Nonsteady Burning and Combustion Stability of Solid Propellants*, AIAA, Washington, D.C., 1992, Chaps. 7, 14.

S. Son
Associate Editor